

《Original》

## Utilization of the Stand-by Fuel Assemblies

Hark Rho Kim and Chang Hyun Chung

Seoul National University  
(Received February 18, 1981)

### 예비 핵연료의 이용

김 학 노 · 정 창 현

서울대학교  
(1981. 2. 18 접수)

#### Abstract

The change in the design-basis refueling strategy caused by the unexpected nuclear fuel failures may result in discharging intact fuel assemblies which were irradiated in the positions symmetric to the failed ones in addition to the failed ones in order to maintain the symmetric power shape in the reactor core. In this work an attempt is made to reuse the intact fuel assemblies which were discharged before reaching the design burnup in the above-described situation so as to improve the fuel utilization. The TDCORE code is used to estimate the flux and power distribution, and the RELOAD-II code for searching the optimal loading pattern with the minimum assembly radial power peaking factor. For the case of the Ko-ri unit 1, its third cycle burnup could be extended to 11,648 MWD/MTU by reusing the four low-burned fuel assemblies removed at the end of the first cycle, and then the loading pattern is searched to the equilibrium cycle.

#### 요 약

핵연료 집합체의 예기치 않은 파손으로 인하여 설계 근거 재장전 방침이 변경되면 원자로심 내에서의 출력 분포 비균형을 막기 위하여 파손된 핵연료 집합체 이외에 대칭 위치의 집합체도 제거되어야 할 경우가 있다. 이와 같은 때에 제거된 핵연료 집합체가 설계연소도에 미달되는 경우 이를 다시 사용하여 핵연료 이용률을 증진시키는 것이 연구되었다. TDCORE 코드가 노심 해석을 위해 이용되었으며, 최적장전모형을 찾는 코드로는 RELOAD-II가 이용되었다. 고리 1호기에 적용한 결과, 제 1주기말에 제거된 비교적 적게 연소된 4개의 핵연료집합체를 제 3주기에서 이용할 경우 주기 연소도가 11648 MWD/MTU(가동율: 80%)에 이를 수 있음을 알 수 있었으며 평형주기까지의 장전모형을 추적하였다.

#### 1. Introduction

One of the most important aspects in

the operation of the nuclear power plant is the in-core fuel management, in which the fuel loading with the minimum power peaking factor is often the primary consi-

deration in view of safety.

Recent attempts have been made to optimize the reactor fuel loadings, although they are not always satisfactory from the standpoint of minimizing the power peaking factor. Various optimization techniques have been used in these attempts, including the linear programming, the non-linear programming, the dynamic programming, the variational methods, the heuristic learning techniques, and the direct-search techniques. Most of these methods are not used as a single method, but combination of such methods in different approximations for various scope of decisions. Until now, by using the previously-described methods, the design-basis refueling strategies have been investigated under the assumption that the reactor would be operated as planned.

In this work, however, the refueling strategy of a PWR with the operational problems induced by the fuel failures is studied and especially the reuse of the low-burned fuel assemblies, presently stored in the pool, is attempted to improve the fuel utilization. It is to be emphasized that the reuse of these stand-by fuel assemblies is limited within the constraint of maintaining the quarter-core symmetry of the power distribution in the reactor core from the viewpoint of the reactor safety.

The TDCORE<sup>1)</sup> code, which uses the Børresen approximation<sup>2)</sup> and the albedo-type boundary condition<sup>3)</sup>, is adopted to determine the power distribution in the reactor core. The RELOAD-II code, which is a modified version of the RELOAD code<sup>4)</sup>, is utilized as a search code of the optimal loading pattern with the minimum power peaking factor at the beginning of the cycle. The Ko-ri unit 1 is chosen as a

reference power plant.

## 2. Optimization Approach

Since the nuclear calculations associated with any optimization procedure are repeated, some sacrifice in the accuracy of the model must be made to acquire the necessary speed. Thus the Børresen's approximation<sup>2)</sup> is applied to the two-group diffusion equation. The two-group diffusion equations in the  $x$ - $y$  geometry are

$$\begin{aligned} -\nabla \cdot D_1 \nabla \phi_1 + (\Sigma_{a1} + \Sigma_r + D_1 B_z^2) \phi_1 \\ = \frac{1}{K_{eff}} (\nu \Sigma_{f1} \phi_1 + \nu \Sigma_{f2} \phi_2) \end{aligned} \quad (1)$$

$$-\nabla \cdot D_2 \nabla \phi_2 + (\Sigma_{a2} + D_2 B_z^2) \phi_2 = \Sigma_r \phi_1 \quad (2)$$

After integrating Eqs. (1) and (2) over the mesh volume and applying the Børresen's approximation<sup>2)</sup> to the midpoint flux in a node, the finite difference equations have the following form:

$$-\sum_j \phi_g^{ij} + Q_g^{ij} \phi_g^{ij} = S_g^{ij} \quad (3)$$

While Eq. (3) is for interior nodes, the revisions for the node at the core boundary must be provided. When Eqs. (1) and (2) are modified, we obtain a revision of Eq. (3) for the node at the core boundary.

$$-\sum_j^{4-n_r} \phi_g^{ij} + Q_g^{ij} \phi_g^{ij} = S_g^{ij} \quad (4)$$

Where  $ij$  indicates the mesh point under consideration,  $ij$  denotes the mesh point adjacent to  $ij$ , and  $n_r$  is the number of the faces surrounded by the reflector. The physics of the core-state model is described in details in the TDCORE code.<sup>1)</sup>

The following assumptions are made to make the minimized power peaking factor be the main decision variable for an optimal loading pattern:

1. The minimum radial assembly power peaking factor at the beginning of the cycle (ROC) results in the optimal loading pat-

tern, since the 3-dimensional analyses or the pin-by-pin 2-dimensional calculations are insurmountable in view of computer cost.

2. The quarter-core symmetry is maintained. Therefore the fuel assemblies being reused to improve the fuel utilization must be located within this constraint.

3. The reactor is divided into three distinct regions: the periphery region, the intermediate region, and the interior region which is subdivided into two position types of the odd and the even parity. In the even-parity position, the sum of the  $ij$  index is even, while it is odd in the odd-parity position. The fresh fuel assemblies are always loaded in the periphery region and are not shuffled in the optimization search. The fuel assembly in the intermediate region may be shuffled with any other fuel assembly excluding the one on the periphery region. The fuel assembly in the even-parity position is not permitted to exchange with the fuel assembly in the odd-parity position. To illustrate this

arrangement, Fig. 1. shows the visualization of the Ko-ri unit 1 quarter-core.

4. The infinite multiplication factor of each fuel assembly is calculated by using the following formula<sup>4)</sup>:

$$k_{\infty} = \frac{\nu \Sigma_{f1}^{ij}}{\Sigma_{a1}^{ij} + \Sigma_r^{ij}} + \frac{\nu \Sigma_{f2}^{ij}}{\Sigma_{a2}^{ij}} \cdot \frac{\Sigma_r^{ij}}{\Sigma_{a1}^{ij} + \Sigma_r^{ij}} \quad (5)$$

This information on the infinite multiplication factor is used to reduce the computing time by limiting the fuel assembly exchange as follows:

"A fuel assembly of higher reactivity (infinite multiplication factor) is never exchanged with any having the lower reactivity if the latter has the higher power density of the two".

The shuffling logic proceeds in three distinct steps, which is described in details in the RELOAD code.<sup>1)</sup>

### 3. Results and Discussions

The input parameters of the two codes, TDCORE and RELOAD-II, are the number of the fuel assemblies, the number of the fuel assemblies located at the core boundary, the coefficient of the fifth-order polynomial representing the group constants as a function of the burnup of each fuel assembly, the albedo value at the core boundary, and the burnup of each fuel assembly. The group constants for each fuel assembly are calculated by using LEOPARD<sup>5)</sup>/CITATION<sup>6)</sup> and fitted to the fifth-order polynomial by adopting the least square method.

This study for reusing the stand-by fuel assemblies stems from the fact that a few assemblies had been removed at the end of the first cycle of the Ko-ri unit 1 to maintain the power symmetry due to the fuel failures in the first cycle. The loading pattern for the first cycle of the Ko-ri

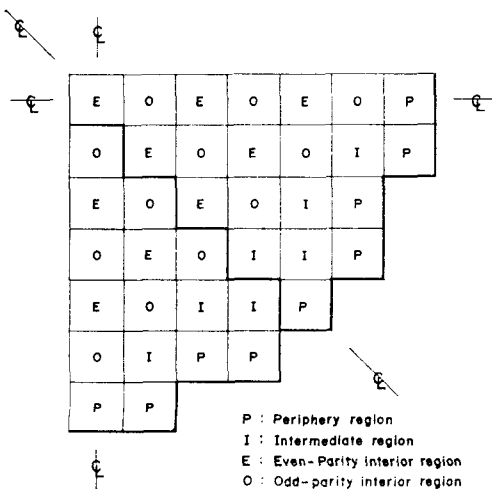


Fig. 1. The Ko-ri Unit 1 One-quarter Core Configuration with Position Designation

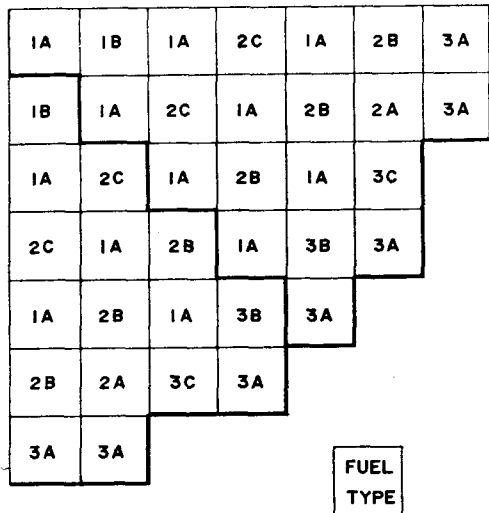


Fig. 2. The One-quarter Core Loading for the First Cycle of the Ko-ri Unit 1

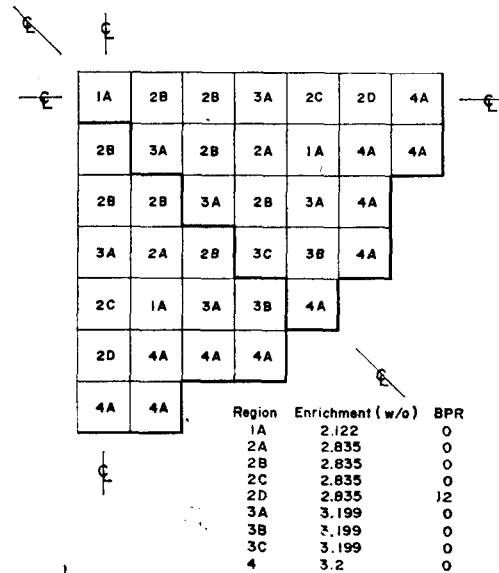


Fig. 3. The Second Cycle Loading Pattern of the Ko-ri Unit 1

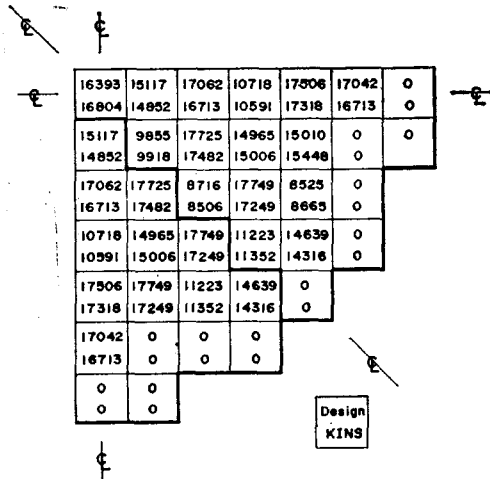


Fig. 4. The Burnup Distribution for the Beginning of the Second Cycle of the Ko-ri Unit 1

unit 1<sup>7)</sup> is shown in Fig.2. Only one fuel assembly with the lowest burnup among the batch 1 fuel assemblies should remain in the second cycle on the design-basis strategy but eight fuel assemblies of the batch 1, which were planned to be discharged at the end of the first cycle, remained

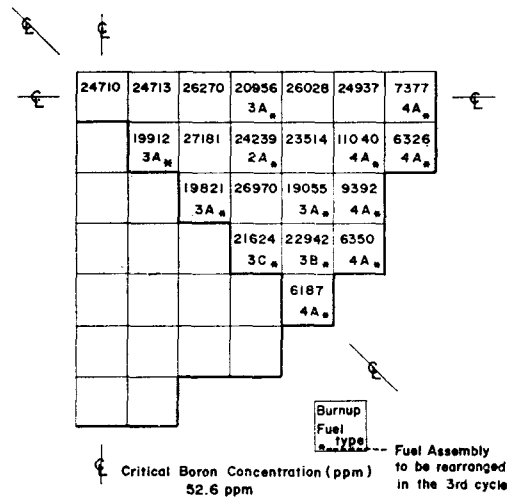


Fig. 5. The Burnup Distribution for the End of the Second Cycle of the Ko-ri Unit 1

in the core instead of those of the batch 3. In Fig.3 the loading pattern is shown for the second cycle of the Ko-ri unit 1 and the design burnup and

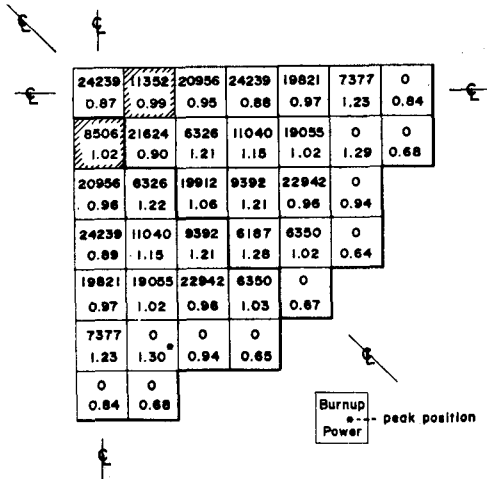


Fig. 6. The Initial Pattern (Case I)

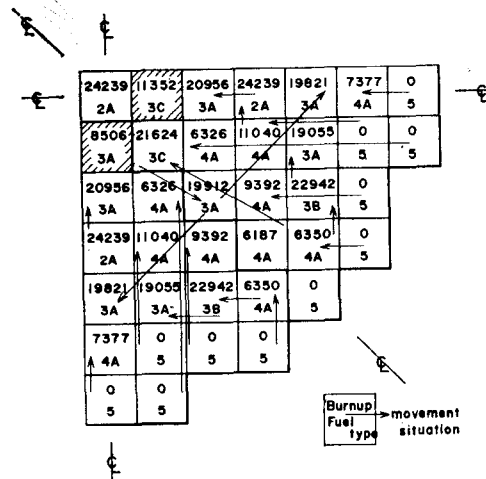


Fig. 7. The Initial Pattern (Case II)

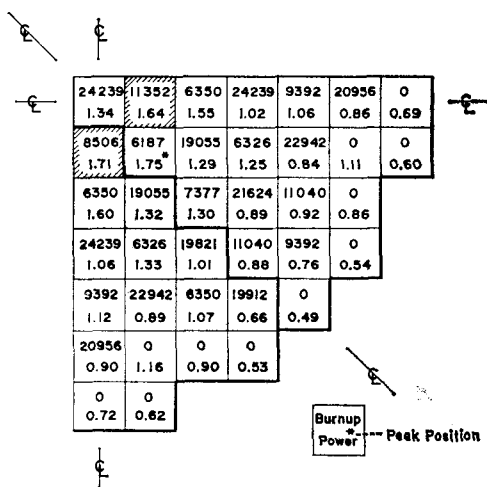


Fig. 8. The Initial Pattern (Case III)

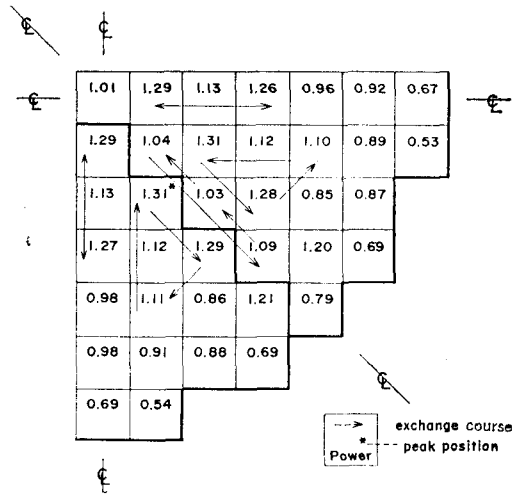


Fig. 9. The Searched Pattern (Case I)

the calculated burnup distribution in each fuel assembly at its BOC is given in Fig. 4. The end of the second cycle burnup in each assembly is expected as in Fig. 5, where the end of the cycle (EOC) is taken when the critical boron concentration is nearly 50 ppm.

The optimization search for the third cycle loading pattern is carried out and

the results are demonstrated in Figs. 6 through 10. Only four fuel assemblies among the eight fuel assemblies removed in the second cycle are reused in the third cycle within the constraint of preventing the power tilt in the core. The location of the reused fuel assemblies must be limited according to the previously-described assumption. 2. The case I in Fig. 6 is the

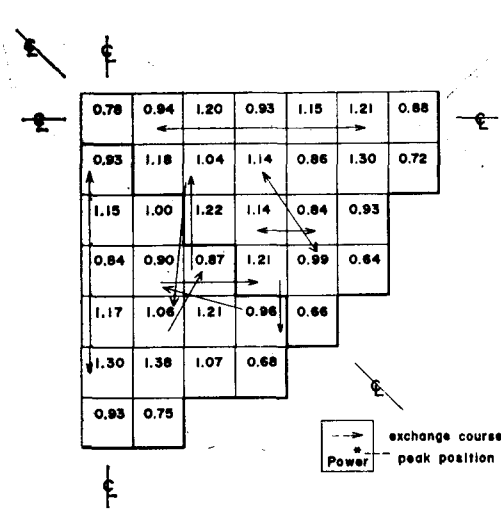


Fig. 10. The Searched Pattern (Case II)

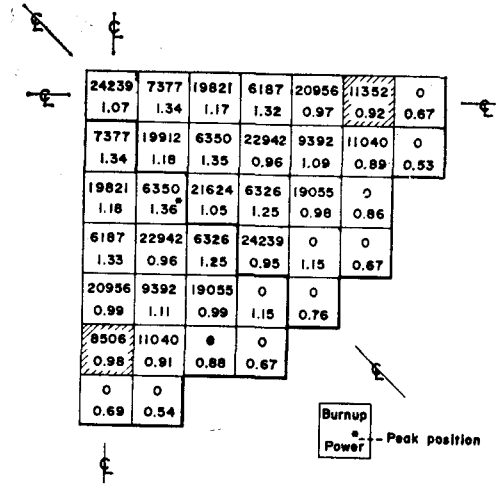


Fig. 11. The Loading Pattern and Burnup Distribution for the Third cycle of the Ko-ri Unit 1, and its Fuel Assembly Movement Situation from the Second Cycle to the Third Cycle

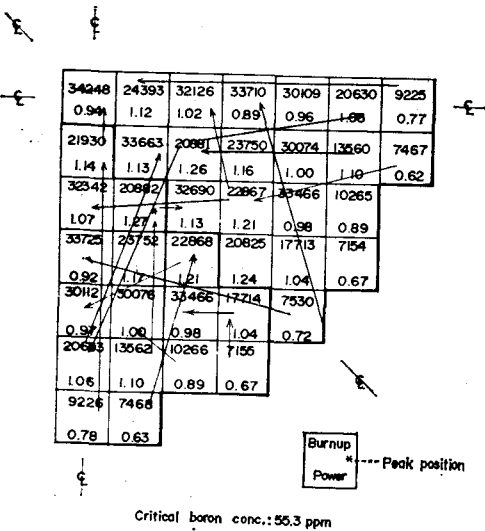


Fig. 12. Ko-ri Unit 1 Cycle 3 EOC Burnup and Power Distribution and Fuel Assembly Movement Feature from the Third Cycle to the Fourth Cycle

checkerboard type loading and searched as in Fig. 9. In Fig. 7 is chosen the case II for lessening the power density in the center region and the pattern does not change through the search procedure. The arbitrary loading pattern is shown in Fig. 8 and its results is given in Fig. 10. The

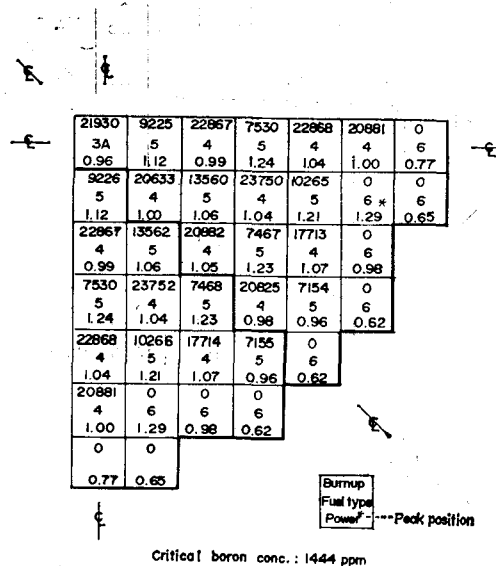


Fig. 13. Ko-ri Unit 1 Cycle 4 Loading Pattern and its BOC Burnup and Power Distribution

arrows in Figs. 9 to 10 represent the movement of the fuel assembly from the initial loading pattern to the searched one. The shaded assemblies indicate the positions

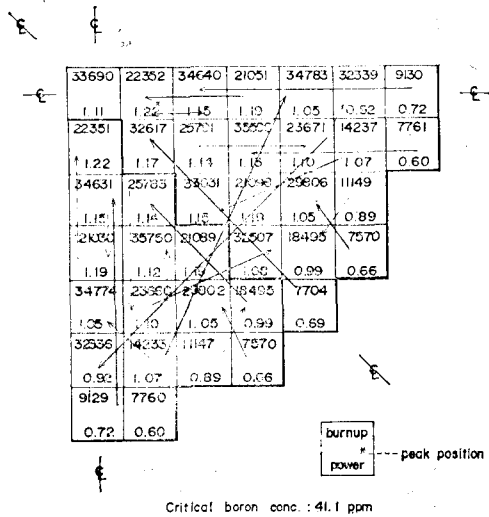


Fig. 14. Ko-ri Unit 1 Cycle 4 EOC Burnup and Power Distribution and Fuel Assembly Movement Feature from the Fourth Cycle to the Fifth Cycle

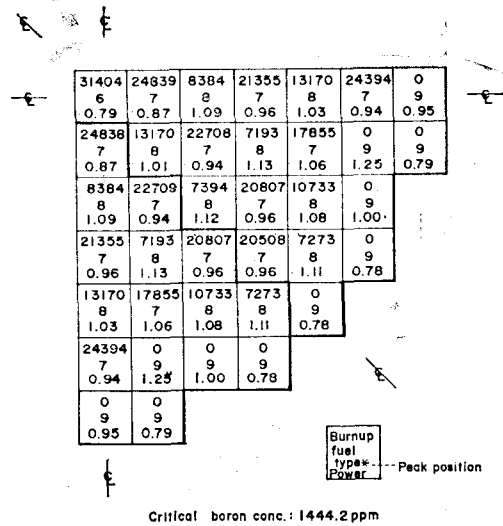


Fig. 15. Ko-ri Unit 1 Cycle 5 Loading Pattern and its BOC Burnup and Power Distribution

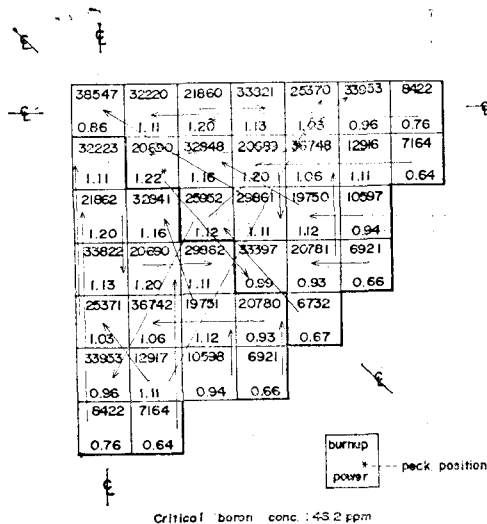


Fig. 16. Ko-ri Unit 1 Cycle 5 EOC Burnup and Power Distribution and Fuel Assembly Movement Feature from the Fifth Cycle to the Sixth Cycle.

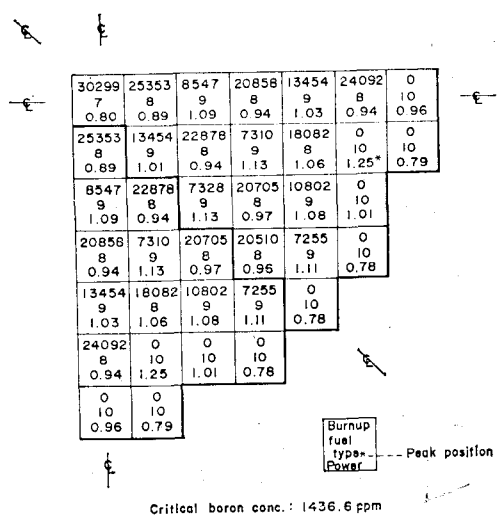


Fig. 17. Ko-ri Unit 1 Cycle 6 Loading Pattern and its BOC Burnup and Power Distribution

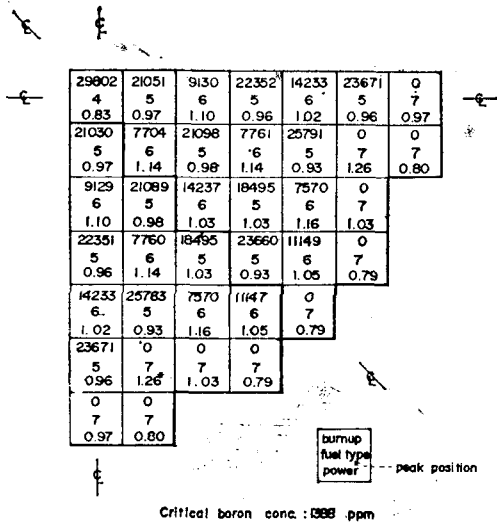


Fig. 18. Ko-ri Unit 1 Cycle 6 EOC Burnup and Power Distribution and Fuel Assembly Movement Feature from the Sixth Cycle to the Seventh Cycle.

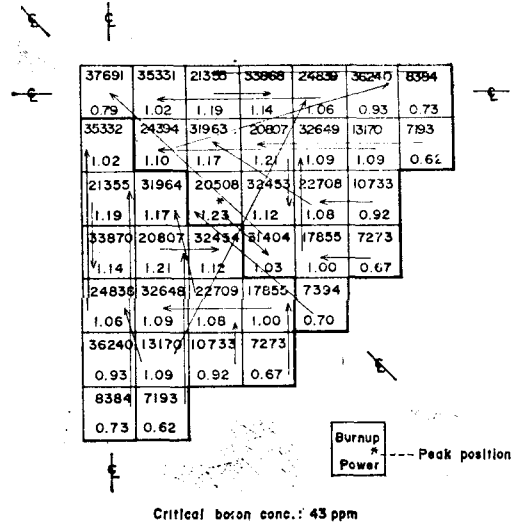


Fig. 19. Ko-ri Unit 1 Cycle 7 Loading Pattern and its BOC Burnup and Power Distribution

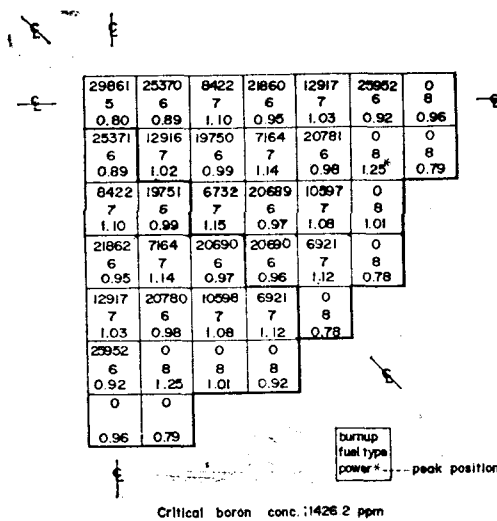


Fig. 20. Ko-ri Unit 1 Cycle 7 EOC Burnup and Power Distribution and Fuel Assembly Movement Feature from the Seventh Cycle to the Eighth Cycle.

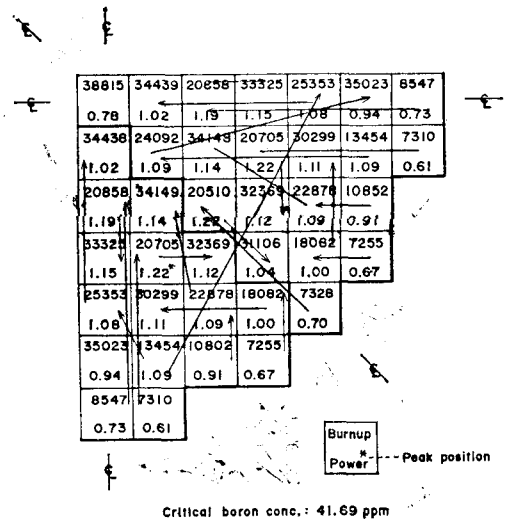


Fig. 21. Ko-ri Unit 1 Cycle 8 Loading Pattern and its BOC Burnup and Power Distribution



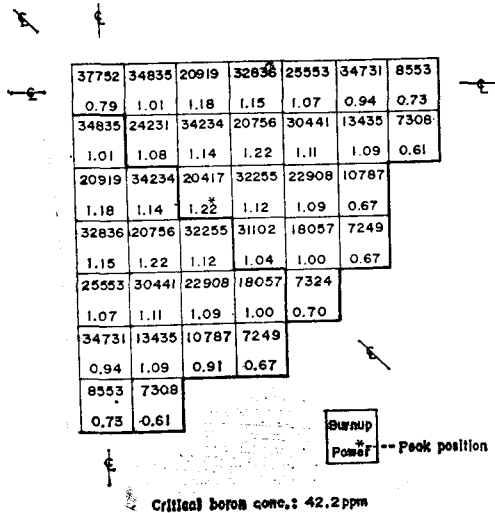


Fig. 22. Ko-ri Unit 1 Cycle 8 EOC Burnup and Power Distribution

of the reused stand-by fuel assemblies in Fig. 6,7,8 and 11. The searched optimal loading pattern is the case II shown in Fig. 7, since it was assumed that the pattern with the minimum power peaking factor is optimal. The fuel assembly movement based on the case II from the second cycle to the third cycle is shown in Fig. 11, where the loading pattern and the burnup for the third cycle are also given. In from Fig. 12 to Fig. 22, the loading pattern, the BOC and EOC burnup and power distribution are provided from the third cycle to the equilibrium cycle. And the batch burnup and the cycle burnup are represented in TABLE.

4. Conclusion

The in-core fuel management is directly

Table. 1. Cycle Burnup for the Batch and the Cycle, Respectively.

Batch Number	Cycle										Discharge Burnup	
	1	2	3	4	5	6	7	8	9	10		
1	16785 (41)	8379 (9)										18624
2	16507 (40)	9292 (40)	9584 (5)									26997
3	10619 (40)	9926 (32)	11510 (36)	11204 (1)								29213
4		8801 (40)	14314 (40)	11371 (40)	8745 (1)							34704
5			9365 (40)	12219 (40)	11082 (40)	7830 (1)						32862
6				9434 (40)	11806 (40)	11467 (40)	7411 (1)					32892
7					9035 (40)	12349 (40)	11369 (40)	7453 (1)				32939
8						9252 (40)	12162 (40)	11322 (40)	7453 (1)			32922
9							9352 (40)	12104 (40)	11322 (40)	7453 (1)		32964
10								9344 (40)	12104 (40)	11322 (40)		32956
11									9344 (40)	12104 (40)		32956
12										9344 (40)		32956
Cycle Avg.	14655	8991	11648	11010	10625	10996	10932	10895	10895	10895		

Note: The number in the parenthesis means the numer of the assemblies.

connected with the power cost, in that it provides the economic operational guide for the nuclear power plant. Thus various methods have been investigated to reduce the power cost. There are numerous methods, including the batch size change method, the feed fuel enrichment change method, the stretch-out operation using the feedback effect of the moderator temperature coefficient, and the method of reusing the low-burned fuel assemblies discharged in the previous cycle, to improve the fuel utilization.

The reuse method is applied to the low-burned fuel assemblies discharged at the end of the first cycle of the Ko-ri unit 1 and these assemblies ( $2 \times 8, 506$  MWD/MTU (3A) and  $2 \times 11, 352$  MWD/MTU (3C)) are reinserted on the quarter-core symmetry axis in the third cycle. As a result the third cycle burnup could be extended to 11,648 MWD/MTU (capacity factor: 80%). And then the loading pattern is searched to the equilibrium cycle.

The overall power and burnup calculation is not considered in search procedure of the optimal loading pattern. In other words, the present model with the emphasis on the minimum power peaking factor at BOC could be improved, if it may include other aspects such as thermohydraulic and neutro

economy features. Thus more intensive studies in this field should be performed.

#### Acknowledgements

The authors would like to thank Prof. Chang Hyo Kim of the Seoul National University for his continuous advice and discussion during this study. Thanks are also due to Mr. Jin Soo Kim of the Korea Advanced Energy Research Institute for providing useful informations.

#### References

1. C.H. Kim et al., "A Study on the Nuclear Fuel Management for Pressurized Water Reactors," College of Engineering, SNU. (1979)
2. S. Børresen, *Nucl. Sci. Eng.*, **44**, 37 (1971).
3. P.C. Karambokas et al., *Nucl. Sci. Eng.*, **61**, 181 (1976).
4. J.J. Duderstadt et al., "Nuclear Reactor Analysis," John Wiley & Sons (1976).
5. R. F. Barry, WCAP-3269-26, Westinghouse Electric Corp. (1963).
6. T.B. Fowler et al., ORNL-TM-2496, Rev. 2, Oak ridge National Lab. (1971).
7. FSAR for the Ko-ri Nuclear Power Plant, Ch. 4, KECO (1977).
8. C.K. Lee et al., "A Review of the Nuclear Fuel Design Change according to the Operational Achievements of the Ko-ri Unit 1", KAERI (1980).